

Fast-timing measurements in $^{95,96}\text{Mo}$

S Kisyov¹, S Lalkovski¹, N Mărginean², D Bucurescu², L Atanasova³,
 D Balabanski³, Gh Cata-Danil², I Cata-Danil², D Deleanu²,
 P Detistov³, D Filipescu², D Ghita², T Glodariu², R Mărginean²,
 C Mihai², A Negret², S Pascu², T Sava², L Stroe², G Suliman², N V
 Zamfir² and M Zhekova¹

¹Faculty of Physics, University of Sofia "St. Kliment Ohridski", Sofia, Bulgaria

²National Institute for Physics and Nuclear Engineering "Horia Hulubei", Magurele, Romania

³Institute for Nuclear Research and Nuclear Energy, Bulgarian Academy of Science, Sofia, Bulgaria

E-mail: stanimir.kisyov@phys.uni-sofia.bg

Abstract. Half-lives of the $19/2_1^+$ and $21/2_1^+$ states in ^{95}Mo and of the 8_1^+ and 10_1^+ states in ^{96}Mo were measured. Matrix elements for yrast transitions in ^{95}Mo and ^{96}Mo are discussed.

1. Introduction

There are twenty six molibdenum isotopes on the Segré chart, studied by means of γ -ray spectroscopy [1]. They span a wide region, where a variety of shapes are observed, from the spherical ^{90}Mo to one of the most deformed nuclei in the $A \approx 110$ mass region. Of particular interest are the $^{95,96}\text{Mo}$ nuclei, which are placed in a region where an offset of the quadrupole deformation takes place [2]. Also, the two nuclei are placed in the third oscillator shell in protons and at the beginning of the fourth oscillator shell in neutrons, where high- j and low- j single particle orbits with $\Delta j = 3$ enhance the effects of octupole collectivity [3]. Being on the edge between the single-particle and collective modes, the two nuclei represent an excellent laboratory, where different approaches can be tested. In this respect, of particular interest are the nuclear lifetimes of excited states which are directly related to transition matrix elements and hence are sensitive to the underlying structure.

2. Experimental Set Up and Data Analysis

Fast-timing measurements were performed in $^{95,96}\text{Mo}$. The nuclei were produced in fusion-evaporation reactions, performed at the NIPNE tandem accelerator. A beam of ^{18}O was accelerated up to 62 MeV and focused on a ^{82}Se target with a thickness of 5 mg/cm² on a 2 mg/cm² thick Au backing. The cross section for the $^{82}\text{Se}(^{18}\text{O}, 5n\gamma)^{95}\text{Mo}$ channel was estimated as 400 mb, while that for the $^{82}\text{Se}(^{18}\text{O}, 4n\gamma)^{96}\text{Mo}$ channel as about 100 mb. The beam intensity was of the order of 20 pA.

The gamma-ray detector system consisted of eight LaBr₃:Ce detectors and eight HPGe detectors, working in coincidence [4, 5]. The LaBr₃:Ce detectors issue positive dynode and negative anode signals. The dynode signals were used for energy measurements while the anode signals were used for timing. The time signals were shaped by Constant Fraction Discriminators

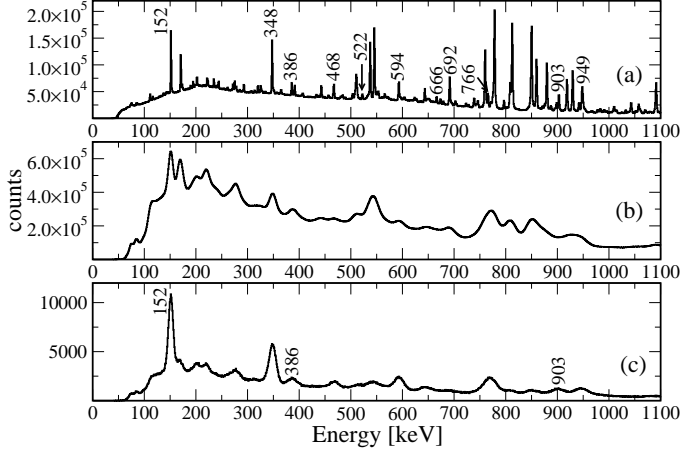


Figure 1. ^{95}Mo energy spectra. HPGe total projection (a), LaBr₃:Ce total projection (b), LaBr₃:Ce energy spectrum gated on 692-keV transition with HPGe detectors (c).

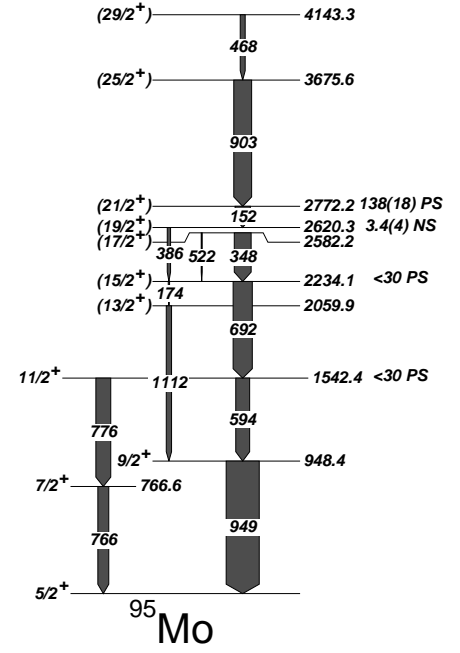


Figure 2. Partial level scheme of ^{95}Mo .

(CFDs) and sent to Time-to-Amplitude-Converters (TACs) operating in a common STOP mode. The energy and time signals were digitized and the data were stored in event files, collected for approximately two hours each. The system was triggered by coincidences between two LaBr₃:Ce and one HPGe detector. The data were analyzed with GASPware and RadWare [6] packages.

Three dimensional matrices were sorted with LaBr₃:Ce energy on two of the axes and a relative time, defined as $T_{1,2} = t \pm (t_1 - t_2)$, on the third axis. Here, t_1 is the moment of interaction of the preceding in the time γ -ray and t_2 is the moment at which the delayed γ -ray was detected. t is an arbitrary offset. If the two γ -rays feed and de-excite a particular nuclear level and E_{γ_1} denotes the energy of the feeding transition, while E_{γ_2} is the energy of the delayed transition, then for each event two matrix elements $(E_{\gamma_1}, E_{\gamma_2}, T_1)$ and $(E_{\gamma_2}, E_{\gamma_1}, T_2)$ were incremented. Then, from the time projected $(E_{\gamma_1}, E_{\gamma_2})$ and $(E_{\gamma_2}, E_{\gamma_1})$ two-dimensional gates, two time spectra, symmetric with respect to the arbitrary offset t , were obtained. If the lifetime of the level of interest is of the order of the detectors time resolution, the centroids $C_D = \langle t \rangle = \int tD(t)dt / \int D(t)dt$ of the time distributions will be displaced by 2τ one from the other, where τ is the lifetime of the level. This procedure is known as the centroid shift method [7,8]. It should be noted that the two centroids will overlap in the cases where E_{γ_1} and E_{γ_2} feed and de-excite nuclear level with a lifetime shorter than the binning of the converter, which was of 6 ps/channel. For lifetimes longer than the detector time resolution the slope method was used to determine level lifetimes. To reduce the background in the LaBr₃:Ce spectra, the $(E_{\gamma}, E_{\gamma}, T)$ matrices were incremented after an (E_{γ}, T) gate was implied on any of the HPGe detectors.

Sample energy spectra, obtained with HPGe and LaBr₃:Ce detectors, are presented in Fig. 1. Fig.1(a) shows a total energy projection for all HPGe detectors. Peaks corresponding to transitions in ^{95}Mo are denoted with the transition energies. Fig 1(b) presents the total energy projection obtained with all LaBr₃:Ce detectors. A LaBr₃:Ce spectrum, gated on the 692-keV transition in ^{95}Mo in the HPGe detectors is shown on Fig. 1(c).

The partial level scheme of ^{95}Mo presented on Fig. 2 is based on the coincidence measurements

Table 1. Energy levels and transitions in ^{95}Mo .

J^π [†]	E_{level}^a [keV]	E_γ^b [keV]	I_γ	λM [†]	$T_{1/2}$
5/2 ⁺	0.0				stable
7/2 ⁺	766.6(7)	766.3	0.80(16)	M1+E2	4.4(7) ps [†]
9/2 ⁺	948.4(7)	948.7	2.4(5)	E2(+M3)	2.58(11) ps [†]
11/2 ⁺	1542.2(10)	593.6	1	M1+E2	≤30 ps
11/2 ⁺	1542.2(10)	775.7	1.09(22)	E2	≤30 ps
(13/2 ⁺)	2060.2(17)	1112.0		(E2)	
(15/2 ⁺)	2234.2(15)	173.8	0.086(10)	(M1+E2)	≤30 ps
(15/2 ⁺)	2234.2(15)	692.0	1.39(25)	E2	≤30 ps
(17/2 ⁺)	2582.4(16)	348.1	1.23(11)	M1(+E2)	d
(17/2 ⁺)	2582.4(16)	522.1	0.062(12)	[E2] ^c	d
(19/2 ⁺)	2620.5(16)	38.1 [†]	0.056	[M1+E2] ^c	3.4(4) ns
(19/2 ⁺)	2620.5(16)	386.4	0.23(2)	E2	3.4(4) ns
(21/2 ⁺)	2772.4(17)	152.3	1.1(5)	M1	138(18) ps
(25/2 ⁺)	3675.8(20)	903.4	1.3(3)	E2	d
(29/2 ⁺)	4143.5(23)	467.7	0.37(5)	E2	d

[†]from NNDC [9], unless otherwise noted; ^afrom a least-squares fit to E_γ ; ^buncertainty of 1.0 keV; ^cfrom the J^π difference; ^dno enough statistics in the present experiment.

performed in the present study and is consistent with the level scheme presented in ref. [10]. Nuclear level spins and parities J^π , level energies E_{level} , γ -ray energies E_γ , intensities I_γ and multipolarities λM along with the half-lives $T_{1/2}$ of the respective levels in ^{95}Mo are listed in Table 1. Gamma-ray intensities for the strongest yrast transitions were deduced from a spectrum gated by the 949-keV transition and normalized to the 594-keV transition. In the cases where a particular level decays by more transitions, spectra gated on the feeding transition were used to normalize the intensity of the weaker transition to the intensity of the strongest transition. Energy and intensity balance was performed.

The lowest lying levels in ^{95}Mo (Fig. 2) have half-lives shorter than the electronics time binning of 6 ps/channel. The centroids of the symmetric time distributions constructed for the 9/2⁺ state (Fig. 3a) overlap within the time binning, which is consistent with the half-life of 2.58(11) ps quoted in NNDC [9].

Fig. 3(b) shows the time distributions, sorted for the 19/2⁺ state in ^{95}Mo . The time spectrum is obtained by gating on 152-keV and 386-keV transitions with the LaBr₃:Ce detectors. In addition, to reduce the background, gates on 949-keV, 594-keV, 692-keV or 766-keV transitions were applied with the HPGe detectors. A half-life of 3.4(4) ns was obtained from the slope of the time distribution. According to NNDC, the 19/2⁺ state decays via two branches with energies of 38 keV and 386 keV. The 38-keV transition is highly converted, and its energy is outside of the detectors range of sensitivity. Hence, the transition was not observed experimentally in the present experiment. Therefore, the intensity of the 38-keV transition was estimated from the intensity balance performed for the 2582-keV level and after evaluation of the levels side feeding. Using the branching ratios obtained from the present data, $B(E2) = 0.12(9)$ W.u. was obtained.

Fig. 3(c) shows symmetric time spectra for the 21/2⁺ state in ^{95}Mo . The spectrum is gated by the 903-keV and 152-keV transitions in the LaBr₃:Ce detectors. To reduce the background, the same HPGe gates as for the 19/2⁺ state were imposed. A half-life of 138(18) ps was obtained from the centroid shift method.

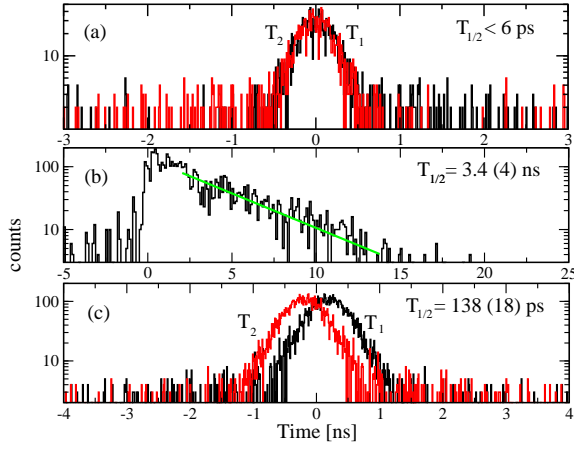


Figure 3. Time spectra for the $9/2^+$ state (a), for the $19/2^+$ state (b), and for the $21/2^+$ state (c) in ^{95}Mo .

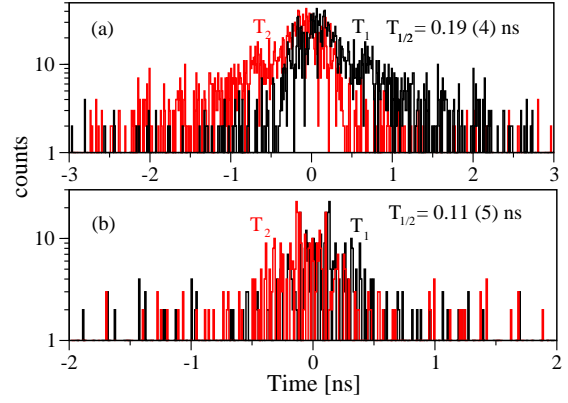


Figure 4. Time spectra for the 8_1^+ state (a) and for the 10_1^+ state in ^{96}Mo .

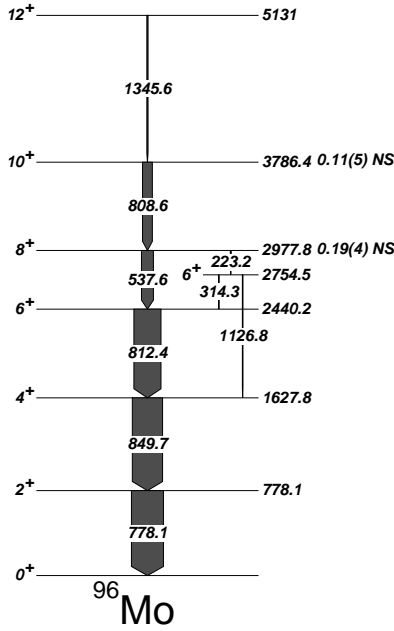


Figure 5. Partial level scheme of ^{96}Mo [11].

A weaker reaction channel leads to the even-even ^{96}Mo nucleus. An analysis similar to the one performed for ^{95}Mo was carried out. Two levels with picosecond half-lives were observed. Fig. 4(a) shows the time distributions obtained for 8_1^+ state in ^{96}Mo . The time spectrum is gated on 809-keV and 538-keV transitions with $\text{LaBr}_3:\text{Ce}$ detectors and on 812-keV transition with HPGe detectors. A half-life of 0.19(4) ns was obtained with the centroid shift method. Hence, the $B(E2; 8_1^+ \rightarrow 6_1^+)$ is 2.3(5) W.u.

Time spectra for the 10_1^+ state in ^{96}Mo are presented on Fig. 4(b). The same gate as in the case of the 8_1^+ state was set on the HPGe detectors. Gates on the 1346-keV and 809-keV

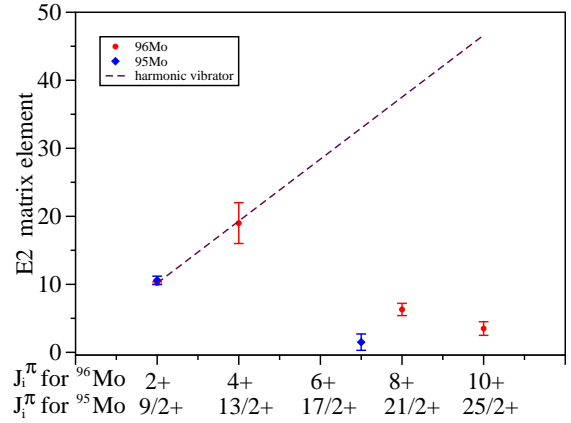


Figure 6. Matrix elements calculated for the $E2$ transitions de-exciting the first five yrast states in ^{95}Mo and ^{96}Mo and compared to the matrix elements, calculated for the harmonic vibrator and normalized with respect to the first phonon in ^{96}Mo .

transitions imposed on LaBr₃:Ce detectors were used to increment the symmetric time spectra. A half-life of 0.11(5) ns was obtained using the centroid shift method. The transition strength for the 809-keV transition results as $B(E2; 10_1^+ \rightarrow 8_1^+) = 0.6(3)$ W.u.

3. Discussion

The ground state of ⁹⁵Mo is a $J^\pi = 5/2^+$ state, which is consistent with the ordering of the neutron single-particle levels in the $A \approx 100$ mass region [12] where $\nu d_{5/2}$ single-particle orbit appears at the beginning of the fourth oscillator shell. Next to the $\nu d_{5/2}$ single-particle orbit is $\nu g_{7/2}$. Indeed, the $J^\pi = 7/2^+$ level, placed at 767 keV in ⁹⁵Mo, decays via a $M1 + E2$ transition to the ground state with $B(E2; 7/2^+ \rightarrow 5/2^+) = 0.96$ W.u [9]. The next yrast $J^\pi = 9/2^+$ level in ⁹⁵Mo has an energy of 948 keV, which is close to the 2_1^+ level energy of the neighboring even-even nuclei. Also, the $9/2^+$ state decays via a strong $E2$ transition with $B(E2) = 11.3(6)$ W.u [9]. Such a state can be interpreted as a $\nu d_{5/2}$ single particle state fully aligned with the first 2_1^+ phonon of an even-even core [13]. In this respect it is interesting to compare the matrix elements, obtained for the $E2$ transitions in the even-even ⁹⁶Mo, with the $E2$ matrix elements, obtained from the yrast transitions in the even-odd ⁹⁵Mo nucleus. The matrix elements, calculated from $|\langle \psi_f || E2 || \psi_i \rangle| = \sqrt{(2J_i + 1) \times B(E2; J_i \rightarrow J_f)}$ for the yrast transitions in ^{95,96}Mo, are shown on Fig. 6. The experimental matrix elements are also compared to the harmonic vibrator matrix elements, which were parameterized from the first excited state in ⁹⁶Mo. The $\langle 2^+ || E2 || 4^+ \rangle$ matrix element, calculated for ⁹⁶Mo [14], remarkably coincides with the harmonic vibrator $\langle 2^+ || E2 || 4^+ \rangle$ matrix element. Also, the $\langle 5/2^+ || E2 || 9/2^+ \rangle$ matrix element, calculated from the ⁹⁵Mo data, is consistent with its interpretation as a fully aligned particle-core coupled state. Further, with the increase of the angular momentum, the experimental matrix elements deviate from the harmonic vibrator description. In fact, the experimental matrix elements are even smaller than the $\langle 0_1^+ || E2 || 2_1^+ \rangle$ matrix element. In this spin range, the odd- and even- mass molibdenum matrix elements are again in the same range. In order to account for the high- J value, these core excited states most probably involve high- j single-particle excitations.

4. Acknowledgments

This work is supported by the Bulgarian Science Fund - contracts DMU02/1, DRNF02/5, DID-02/16, Romanian UEFISCDI - contract IDEI 115/2011 and by a Bulgarian-Romanian partnership contract, numbers DNTS-02/21 and 460/PNII Module III.

References

- [1] NNDC data base (www.nndc.bnl.gov)
- [2] Casten RF, 2000, *Nuclear Structure from a Simple Perspective* Oxford University Press
- [3] Lalkovski S *et al.* 2007 *Phys. Rev. C* **75** 014314
- [4] Mărginean N *et al.* 2010 *Eur. Phys. J. A* **46** 329336
- [5] Kisiov S, *et al.* 2011 *Phys. Rev. C* **84** 014324
- [6] RadWare package (<http://radware.phy.ornl.gov/>)
- [7] Andrejtscheff W *et al.* 1982 *NIM* **204** 123-128
- [8] Régis J-M *et al.* 2010 *NIM A* **622** 83-92
- [9] Basu S K *et al.* 2010 *Nuclear Data Sheets* **111** 2555
- [10] Zang Y H *et al.* 2009 *Phys. Rev. C* **79** 044316
- [11] Chatterjee J M *et al.* 2000 *Nucl. Phys. A* **678** 367-381
- [12] Heyde KLG 1994 *The Nuclear Shell Model*, Springer-Verlag
- [13] de-Shalit A *Phys. Rev.* **122** 1530
- [14] Abriola D *et al.* 2008 *Nuclear Data Sheets* **109** 2501